DIHEDRAL EFFECT FOR STRAIGHT TAPERED AND TWISTED WINGS

P. GILI, Associate Professor
Aeronautical and Space Department, Polytechnic of Turin
Turin - ITALY

Abstract. The dihedral angle of the wing, even if it gives its name to the derivative $C_{l_\beta} = \partial C_l / \partial \beta$, *Dihedral Effect*, (which actually only explains the fact that the aircraft is subjected to a rolling moment L when it is invested by a sideslip angle β) is only one of the elements contributing to C_{l_β}.

Even if a straight wing is invested by a sideslip angle, it can produce a rolling moment. Actually, two wing sections which are equidistant from the symmetrical plane have different distances from the global U-vortex wing system and particularly from the vortices of the tip wing. This is the reason why the induced speed and therefore the induced angle of attack are mostly different on the two semi-wings. This different aerodynamic induction causes a lift difference of the two semi-wings and, therefore, generates a rolling moment. In this case the contribution to C_{l_β} is positive together with a positive sideslip angle.

We have determined the circulation along the wing span and so the induced angle of attack distribution. For this aerodynamic induction we have used a method which allows for the different mutual aerodynamic induction of the two semi-wings each with a different flow situation, again in the presence of a side-slip angle, always through integration along the span.

The results are presented as curves as a function of lift coefficient, and this contribution to C_{l_β} depends on the angle of attack.

Introduction

The derivative $C_{l_\beta} = \partial C_l / \partial \beta$, that is the derivative of the rolling moment coefficient with respect to the sideslip angle, goes under the name of *Dihedral Effect*. This aerodynamic derivative is important, as widely known, in the study of the side- directional motion of the aircraft, and in particular in the determination of its dynamic characteristics concerning Dutch roll and spiral mode.

Among the wing contributions to the C_{l_β}, besides dihedral angle γ, that gives its name to its derivative, we must consider the swept angle Λ contribution and the different aerodynamic induction contribution of the two semi-wings.

Another wing element contribution to C_{l_β} is the shape of the tip of the wing. Anyway, this contribution can be omitted even when the wing has winglets.

Besides the wing, the vertical tail contributes considerably, as we know, to the C_{l_β}, as well as the wing-body relative position, but at a lower degree.

If external bodies, like nacelles or floats, which differ from the fuselage, are fastened to the aircraft, when a sideslip angle is present, they are subjected to a side force. If it has a lever arm with a certain entity from the x-axis, even in this case a rolling moment will be generated. However, these contributions are usually omitted, except when the aircraft has a particular shape.

Among these contributions, three of them have the same order of size: swept wing angle, dihedral wing angle and vertical tail, which can reach at the most same tenth (obviously with angles of a certain entity and conventional vertical tail). The wing aerodynamic induction contribution is of a smaller size (and in any case it depends on the C_L of flight), while the wing-body relative position contribution is of two order smaller, and the contribution of the shape of the tip of the wing is even of three order smaller.

Various authors [4, 6, 8] have worked out simple formulas in order to estimate some of these contributions to C_{l_β} and in particular the most important ones, but among ones however important they have almost always disregarded the contribution of the different aerodynamic induction of the two semi-wings.

A previous study [5] (presented at 19th ICAS Congress in Anaheim), was designed to fine tune a method for evaluating the contribution of the sweep-back angle and of the aerodynamic induction of the wing on the dihedral effect. We evaluated these two contributions to C_{l_β} in two different ways. For the sweep-back angle contribution, we have used a simple integration method along the span of the single infinitesimal wing element, obviously evaluating the

different influences on the two semi-wings when the aircraft is invested by a sideslip angle. For the aerodynamic induction we have used a method which takes into account, also through integration along the span, the different circulation of the two semi-wings, each one with a different situation, again in the presence of a sideslip angle. This method is Anderson's method [1] modified by us for wings of whatever plant form and with any geometric twist. The induced angle of attack α_i has been calculated by using the Anderson relation, and its distribution along the wing span has been simply changed because of the presence of β, by means of a suitable translation along y and a suitable wing tips adjustment, depending on the form of the said wing tip.

In this work, the Anderson method is simply used to define an easy-to-use expression of the Γ circulation of the Prandtl integral-differential equation. Γ, as already known, is expressed by introducing the Fourier series expression, whose coefficients (which are the same for the two semi-wings) have been defined by Anderson. So the different aerodynamic induction on the two semi-wings is calculated while considering the contributions of the wake vortices, as will be further detailed, and adapting the usual Biot and Savart formulas. If we have the distribution of C_L along y, the single infinitesimal wing element contributions must be added to the C_l: this way the C_{l_β} will be easily evaluated as a function of lift coefficient C_L, being this contribution to C_{l_β} dependent on the different circulation of the two semi-wings and therefore depending on the angle of attack.

Problem Formulation

The following method is based on the study of wings with finite aspect ratio, according to Prandtl classic model. When the wing geometry is known, all the other aerodynamic quantities can be deducted from the Γ circulation in every wing section. The Γ function can be determined by solving the Prandtl integral-differential equation:

$$\Gamma(y) = k(y)\,\pi\,V_\infty\,c(y)\cdot[\alpha_a(y) - \alpha_i(y)] \qquad (1)$$

where the k coefficient, which adjusts the theoretical value 2π of the lift angular coefficient, will be a function of y if the wing has a variable section. The other terms, which can be easily understood, can be found in the *List of symbols*.

α_i is the value of the induced angle of attack, which has the following expression:

$$\alpha_i(y) = \frac{1}{4\pi V_\infty}\int_{-b/2}^{b/2}\frac{\frac{d\Gamma'}{dy'}}{y-y'}\,dy' \qquad (2)$$

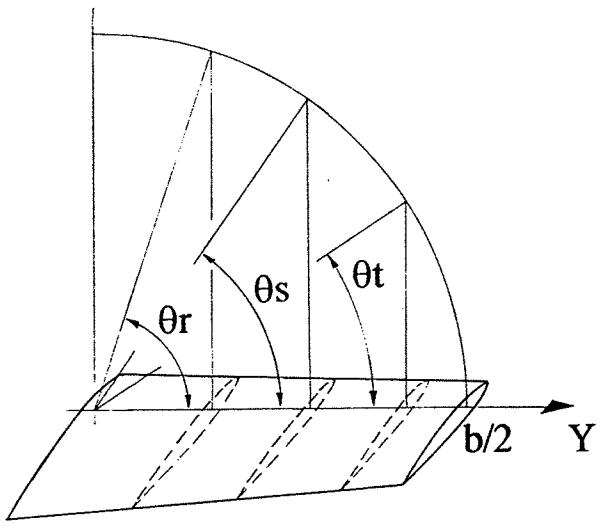

Figure 1: Reference system used by Anderson.

where the y co-ordinate is referred to the point where the induction is calculated and the y' is relative to the inducting vortex.

This equation is not easy to be solved, so that different methods of calculations have been devised, and they have led to the solution of the problem with excellent results, even if with some approximations. In this work, the method which has been used follows the Anderson process in its initial part, as modified in my previous work (see citegili) to eliminate some limitations and to adapt it to any shape of wings and to any twist laws.

The Anderson method replaces the Γ function with its series development and stops the series at a certain N value. The variable must be changed:

$$y = \frac{b}{2}cos(\theta) \qquad (3)$$

As shown in the Fig.1, the $\Gamma(y)$ circulation changes as it follows:

$$\Gamma(\theta) = 2\,b\,V_\infty\,g(\theta) \qquad (4)$$

For a wing with any lift distribution, we can put:

$$g(\theta) = \sum_{n=1,3,5\ldots}^{\infty} A_n\,\sin(n\theta) \qquad (5)$$

with the condition: $g(0) = g(\pi) = 0$.

The lift being generated from an elementary segment dy of wing, which is linked to the circulation Γ by the following relation:

$$dL = \rho\,V_\infty\,\Gamma\,dy \qquad (6)$$

the local lift coefficient can be defined in the following way:

$$c_l = \frac{4b}{c}\,g(\theta) = \frac{4b}{c}\sum_{n=1,3,5\ldots}^{\infty} A_n\,\sin(n\theta) \qquad (7)$$

where c is the local chord (connected with the coordinate y).

If the twist has a linear flow, this will be the proper relation:

$$\alpha_a = \alpha_{as} + \varepsilon^{rad} \mid \cos(\theta) \mid \qquad (8)$$

Notice that α_a is the apparent angle of attack with which the flow invests the section, and the induced angle of attack must be subtracted from it in order to obtain the effective angle of attack α_e, according to the following relation:

$$\alpha_i = \alpha_a - \alpha_e = \alpha_a - \frac{c_l}{m_o} \qquad (9)$$

By applying the Prandtl equations, with all proper replacements, the equation (8) can be rewritten in the following way:

$$\sum_{n=1,3,5...}^{\infty} A_n \sin(n\theta) \left[\frac{n}{\sin\theta} + \frac{4b}{c\, m_o} \right] = \alpha_{as} + \varepsilon^{rad} \mid \cos\theta \mid \qquad (10)$$

This equation can be solved by cutting off the series at a certain number N of terms, the corresponding values of θ being known. This way the result will be a system of N equations in N unknown values like the following ones:

$$A_1\, c_{i1} + A_3\, c_{i2} + \ldots\ldots + A_{(2N-1)}\, c_{iN} =$$

$$= \alpha_{as} + \varepsilon^{rad} \mid \cos(\theta_i) \mid \quad con: \; i = 1, N \qquad (11)$$

where the coefficients c_{ij} are nothing but a function of the parameters m_o, b/c and θ. By performing the following replacement:

$$A_n = B_n \alpha_{as} + C_n \varepsilon^{rad} \qquad (12)$$

you will obtain two systems of N equations in N unknown values, where the unknown values are now B_n and C_n:

$$\begin{aligned} &B_1 c_{i1} + B_3 c_{i2} + \ldots\ldots + B_{2N-1} c_{iN} = 1 \\ &C_1 c_{i1} + C_3 c_{12} + \ldots\ldots + C_{2N-1} c_{iN} = \mid \cos(\theta_i) \mid \qquad (13) \\ &\qquad\qquad with: \quad i = 1, N \end{aligned}$$

Then, the first problem we have faced has been the determination of the N value, in order to obtain good results avoiding lengthy calculations. After few experiments, the number of the N sections and the criterion of angle subdivision have been defined. This criterion provides an increase of the subdivisions of the wing tips, which are the areas where the biggest calculation problems occur. Once the B_n and C_n are known, it's time to calculate A_n and then all the other requested parameters.

The aim of this research being the calculation of the dihedral effect on any type of wings, some calculation programs have been formulated. They had to allow for the geometrical shape of the wing and particularly the tapering, the aspect ratio, the twisting and the wing tip shape; moreover, it might have been possible to prolong the treatment and also discuss about swept angles wings and dihedral angles wings.

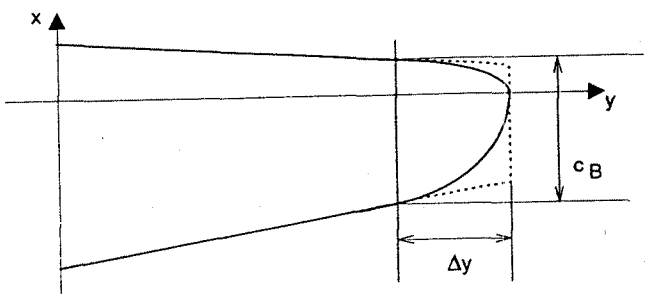

Figure 2: Wing tip shape.

The wing tips can be rounded in any way: an exponential trend can be linked to the rectilinear trend of the trailing and of the leading edge, beginning from a given point along the span. The point at issue is defined as a percentage of the span: $B = \Delta y/(b/2)$ or as a percentage of the mean geometric chord: $B' = \Delta y/c_m = AB/2$ (Fig.2). c_B is the chord connected with the point where the rounding begins, and it will be known once B or B' have been defined.

This program can consider any type of wing tip geometry. By changing the wing geometry, the value of the coefficients of the N system of N equations in N unknown values also changes, because these coefficients are a function of θ, m_o and of b/c, as noticed above. Consequently the value of the other parameters which have been calculated will also be modified: for example, the wing lift coefficient and the rolling moment coefficient.

In the following examples of calculation we have also considered the effect of the wing tip rounding: it will be clear that this parameter seem to affect the aerodynamic features concerned and particularly the C_{l_β}.

Calculation Process

The calculation process which has been adopted allows for the fact that the induction of the wake vortices affects the lift coefficient, and therefore the rolling moment coefficient. For the calculation of the induced angle of attack, we have allowed for the Biot-Savart formula, which provides the induced speed value on a generic point P from a stream vortex whose intensity is $d\Gamma$:

$$\vec{V}_P = \int_s \frac{d\vec{\Gamma} \wedge \vec{r}}{4\,\pi\, r^3}\, \sigma\, ds \qquad (14)$$

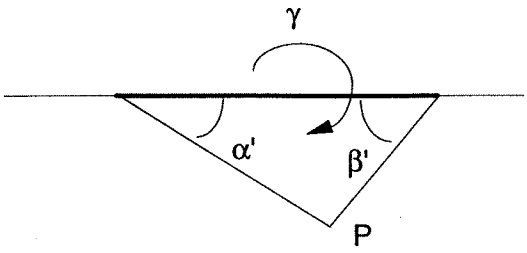

Figure 3: Aerodynamic induction in P point.

About a generic wing, we must consider the contribution of the wake vortices as well as of the adherent vortices to the induction. If the wings are straight, the adherent vortices will result to be "packaged" on the quarter line chord on the basis of Prandtl scheme, so that there will be no contribution of this type of vortices to the total induction. About the swept wings and/or wings with dihedral angle and/or wings whose quarter line chord is not linear, it must be said that this contribution is present, but the following treatment will not allow for it. In fact, because of the symmetry between the two semi-wings, the adherent vortices of any semi-wing induce one another in the same way, apart from the fact that the wing is invested or not by a sideslip angle. Therefore, the contributions of the two semi-wings to the rolling moment are both equal and opposed, and consequently there is no global contribution to the dihedral effect.

If we consider a linear vortical segment with elementary circulation $d\Gamma$, the induced speed on a point P will be the following one:

$$dV_i = \frac{d\Gamma}{4\pi r}(\cos\alpha' + \cos\beta') \qquad (15)$$

whose terms are clearly defined on drawing of Fig.3.

Allowing for the equation (4), we will write as follows:

$$d\Gamma(\theta) = 2bV_\infty \sum_{n=1,3,5\ldots}^{\infty} nA_n \cos(n\theta)\, d\theta \qquad (16)$$

Once the induced speed on a point is known, the induced angle of attack can be calculated as follows:

$$d\alpha_i = \frac{dV_i}{V_\infty} \qquad (17)$$

while considering that the sine can be confused with the angle in small angles.

The trend of α_i being known on any point of the quarter line chord, the lift coefficient and the rolling moment coefficient can be calculated by using the following formulas:

$$c_l = m_o\,(\alpha_a - \alpha_i) \qquad (18)$$

and

$$C_l = \frac{1}{4}\int_{-1}^{1} t\, c_l \frac{c}{c_m}\, dt \qquad (19)$$

where $t = y/(b/2) = \cos\theta$, as shown in the equation (3).

About the calculation of α_i, we must consider 3 contributions for every semi-wing:

1. Induction of a semi-wing on the other one.
2. Induction of a semi-wing on itself $\Rightarrow$ contribution of the vortices on the right of the point concerned.
3. Induction of a semi-wing on itself $\Rightarrow$ contribution of the vortices on the left of the point concerned.

Before illustrating the calculation process, it is necessary to examine the conventional signs which are used for the sense of the vortices. The sense is positive when is counterclockwise, and is negative when clockwise. Therefore the wake vortices of the left semi-wing will have an intensity of $-d\Gamma$, while the vortices of the right semi-wing will be of $+d\Gamma$.

The calculation process of the induction on the two semi-wings is the same, but we can find some differences on those equations that have be applied because of the different aerodynamic conditions of the two semi-wings when they are invested by a lateral wind ($\beta \neq 0$). These differences are only of geometrical type, so that the considerations about the right semi-wing can be easily applied to the left one: it is only necessary to give great care in calculating angles and distances.

Induction of a Semi-Wing on the Other Semi-Wing

In referring to the Fig.4 and applying the equations above, the result will be as follows:

$$\alpha' = \frac{\pi}{2} + \beta \quad \Rightarrow \quad \cos\alpha' = -\sin\beta$$

$$r = (y - y')\cos\beta = \frac{b}{2}(\cos\theta - \cos\theta')\cos\beta$$

$$\alpha_i = \frac{(1-\sin\beta)}{\pi\cos\beta} \sum_{n=1,3,5\ldots}^{2N-1} nA_n \int_{\pi/2}^{\pi} \frac{\cos(n\theta')}{\cos\theta' - \cos\theta}\, d\theta' \qquad (20)$$

In this case the vector dV_i is positive, according to z, and that is why it gives a positive contribution to the total induction on the right semi-wing.

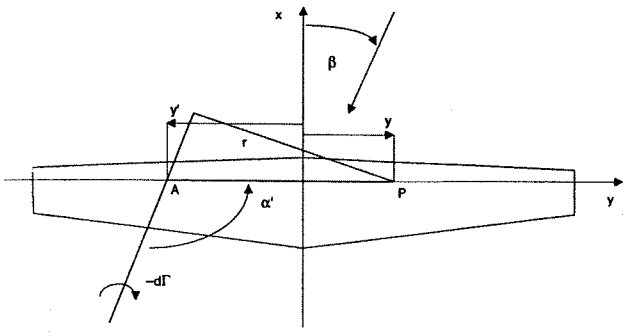

Figure 4: Induction of the vortices of the left semi-wing on the right semi-wing.

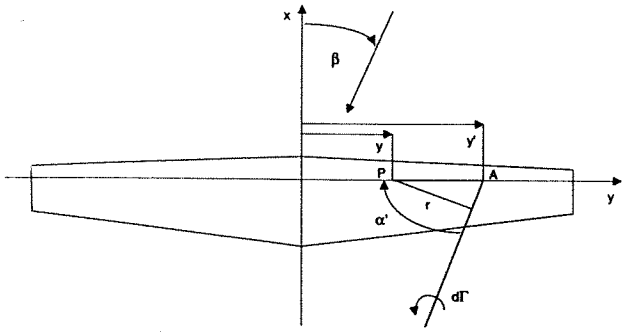

Figure 5: Induction of the vortices of the right semi-wing on itself. Contribution of the vortices on the right of the point concerned.

Induction of a Semi-Wing on Itself ⇒ Contribution of the Vortices on the Right of the Point Concerned

In referring to the Fig.5 and applying the equations above, the result will be as follows:

$$\alpha' = \frac{\pi}{2} - \beta \quad \Rightarrow \quad \cos\alpha' = +\sin\beta$$

$$r = (y' - y)\cos\beta = \frac{b}{2}(\cos\theta' - \cos\theta)\cos\beta$$

$$\alpha_i = \frac{(1+\sin\beta)}{\pi\cos\beta} \sum_{n=1,3,5...}^{2N-1} n\,A_n \int_0^{\theta} \frac{\cos(n\theta')}{\cos\theta' - \cos\theta}\,d\theta' \tag{21}$$

In this case the vector dV_i is positive, according to z, and that is why it gives a positive contribution to the total induction on the right semi-wing.

Induction of a Semi-wing on Itself ⇒ Contribution of the Vortices on the Left of the Point Concerned

In referring to the Fig.6 and applying the equations above, the result will be as follows:

$$\alpha' = \frac{\pi}{2} + \beta \quad \Rightarrow \quad \cos\alpha' = -\sin\beta$$

$$r = (y - y')\cos\beta = \frac{b}{2}(\cos\theta - \cos\theta')\cos\beta$$

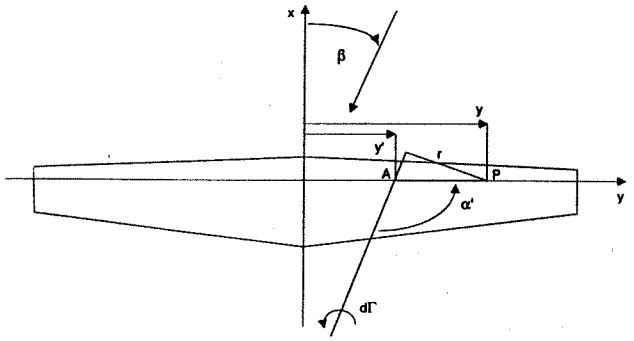

Figure 6: Induction of the vortices of the right semi-wing on itself. Contribution of the vortices on the left of the point concerned.

$$\alpha_i = \frac{(1-\sin\beta)}{\pi\cos\beta} \sum_{n=1,3,5...}^{2N-1} n\,A_n \int_{\theta}^{\pi/2} \frac{\cos(n\theta')}{\cos\theta' - \cos\theta}\,d\theta' \tag{22}$$

In this case the vector dV_i is negative, according to z, and that is why it gives a negative contribution to the total induction on the right semi-wing.

Infinite Induced Speeds Problem

During the calculation of the integrals, which have been illustrated in the previous paragraphs, we had to avoid that the induction would assume an infinite value when calculating the induction of a vortex on itself, that is when $\theta = \theta'$. This condition is unacceptable on a physical point of view, therefore, as suggested by many texts and, as already applied in some other cases [3], it has been decided to replace the hyperbolic function with a straight line, starting from a given value of the integrating function up to the abscissa which corresponds to the vortex axis, as shown in the Fig.7.

Up to the r' which corresponds to the maximum value chosen, the Biot-Savart relation is correct, as follows:

$$dV_i \propto \frac{1}{r} \quad if\ r \to 0 \quad \Rightarrow \quad dV_i \to \infty$$

From r' up to r_o (vortex axis):

$$dV_i \propto \frac{dV_{i_{MAX}}^2}{r' - r_o}(r - r_o) \quad if\ r \to r_o \quad \Rightarrow \quad dV_i \to 0$$

Results and Numerical Examples

C_L Trends

Starting from the relations above, we have done a numerical example based on a wing and having an aspect ratio equal to 7 as well as a taper ratio $r = c_t/c_r$

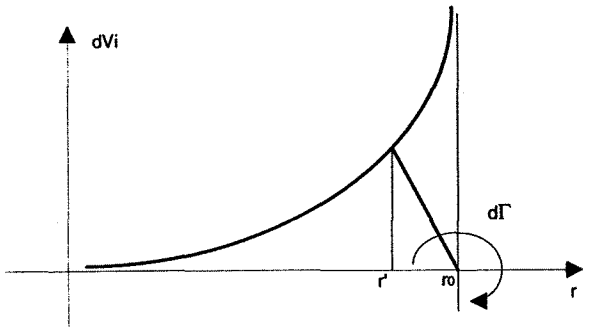

Figure 7: Trend of the vortex induced speed as a function of the distance from the vortex itself.

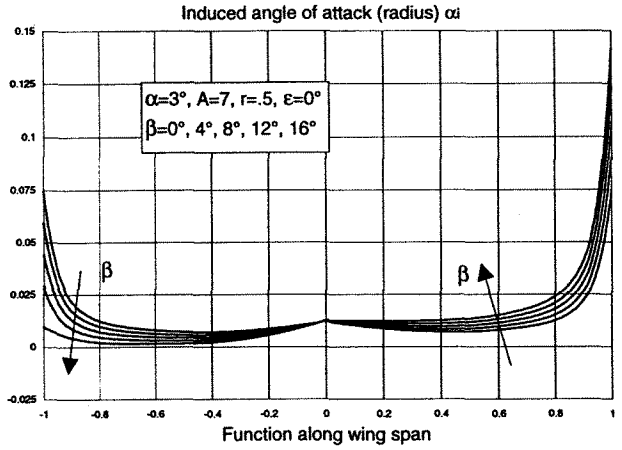

Figure 8: Induced angle of attack along the wing span.

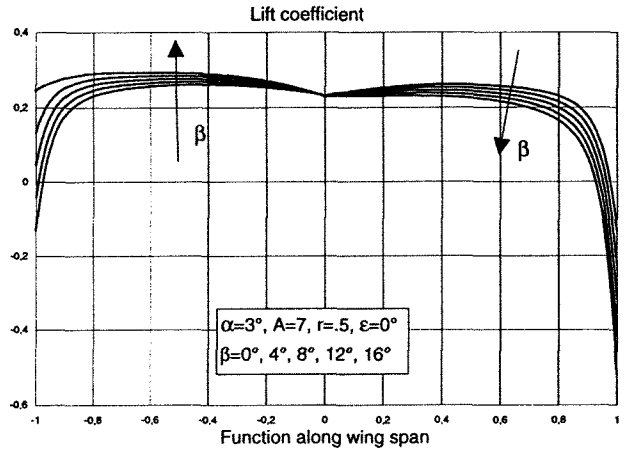

Figure 9: Lift coefficient along the wing span.

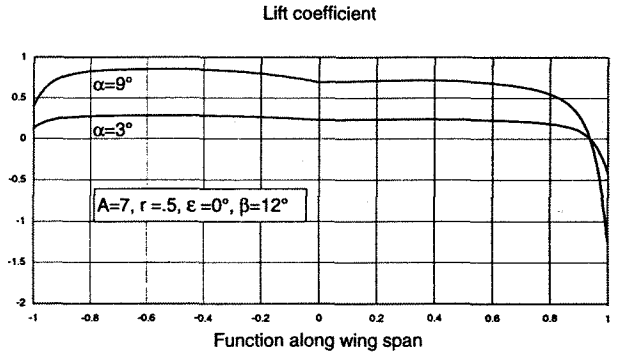

Figure 10: Lift coefficient trend for different α.

equal to 1.0 and 0.5 (that means that the rectangular wing has been used as comparison). For our wing is $\varepsilon^{rad} = 0^o$, so that $\alpha_a \equiv \alpha_{as}$ and $\varepsilon^{rad} = -3^o$ (wing tip pitched negatively). These are the angles of attack α which have been considered: 3^o, 6^o, 9^o and 12^o and the sideslip angles β have been as follows: 4^o, 8^o, 12^o and 16^o, and also, obviously, the situation of the symmetrical flow $\beta = 0^o$.

Here we have some of our results. In the Fig.8 we have reported the induced angle of attack α_i, for the two semi-wings, as a function of y, where the different sideslip angles β have been marked, for $\alpha = 3^o$ and for a wing with the reported features. The different trends on the two semi-wings, because of $\beta \neq 0$ and growing, will be found again, under the form of the lift coefficient C_L, in the Fig.9. These trends also emphasize the rolling moment which is produced and increases with β, just because of the different lift of the two semi-wings.

In the Figs. 10, 11 and 12 the effects, respectively, of the different angle of attack, twist angle and taper ratio have been emphasized by means of the trends of the lift coefficient, which have been compared with the two semi-wings. The other main aerodynamic and geometrical features of the wing are specified in the drawings. The importance of these parameters will be further emphasized on the trends of $C_{l_\beta}(C_L)$.

The effects of the different wing tip shape is evident in the Fig.13: of course the trend of the lift coefficient on the wing tips will only change. The effect of this parameter will be even more evident in the summarizing drawing of the $C_{l_\beta}(B')$.

The C_{l_β} Derivative

Among the several examples which have been shown, we refer now to a particular wing ($A = 7$, $r = 0.5$, $\varepsilon = 0^o$). In the Fig.14 we can show the $C_l(\beta)$ trends for the four values of α above mentioned. As we can see, the function $C_l = C_l(\beta)$ is linear. In consideration of our necessity to obtain a constant value of $C_{l_\beta} = \partial C_l / \partial \beta$, this situation makes our task easier. It is clear that the coefficient of the rolling moment increases both in dependence of α that of β (see Fig.14). Of course, the values of $C_l(\beta)$ are all positive.

The Fig.15 has been reported as a summarizing result: the dihedral effect C_{l_β} has been diagrammatized here as a function of C_L, for three configurations

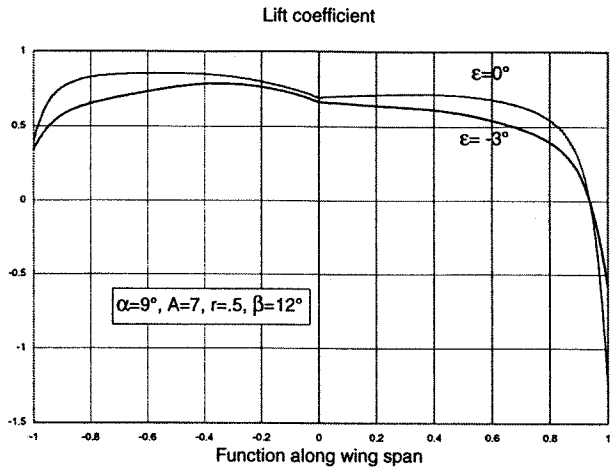

Figure 11: Lift coefficient trend for different ε.

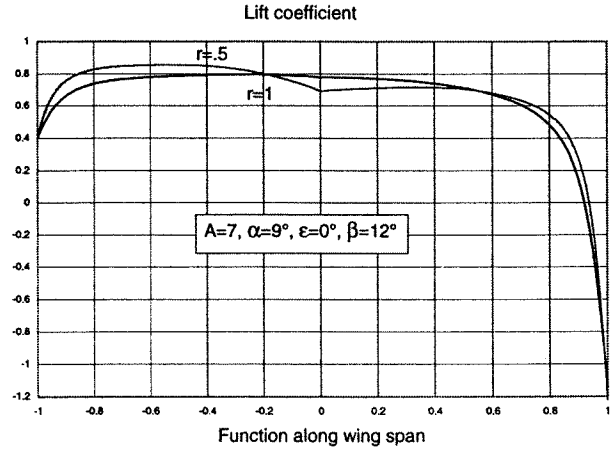

Figure 12: Lift coefficient trend for different r.

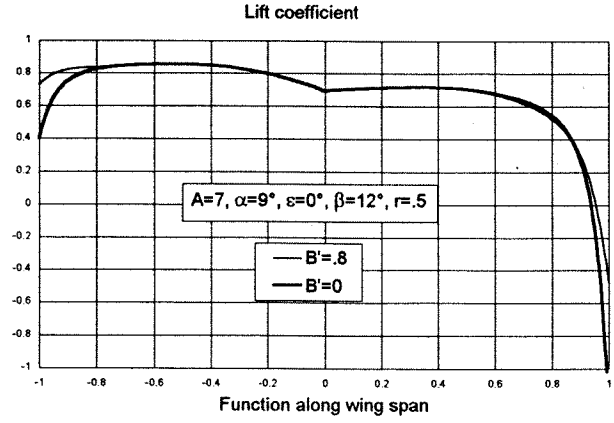

Figure 13: Lift coefficient trend for different B'.

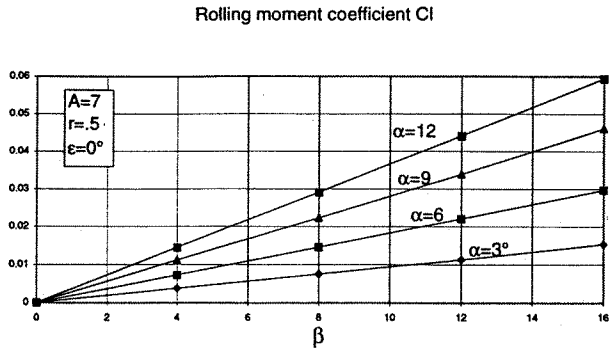

Figure 14: C_l as a function of β for different α.

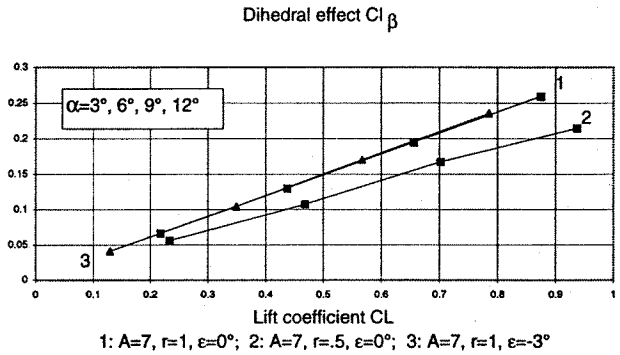

Figure 15: Final results: relation between C_{l_β} and C_L for various configurations.

which differ for one parameter at a time: r or ε. Each curve is formed by four points which refer to the four α above mentioned: the tapering mostly causes the decrease of the C_{l_β} (at a parity of C_L) while the twist translates the curve in parallel as to itself. We have found a perfect linearity of C_{l_β} with C_L.

In the Fig.16 we have reported the effect of the wing tip shape for a tapered wing at two angles of attack: $\alpha = 3^o, 9^o$. The effect is present, but not so evident.

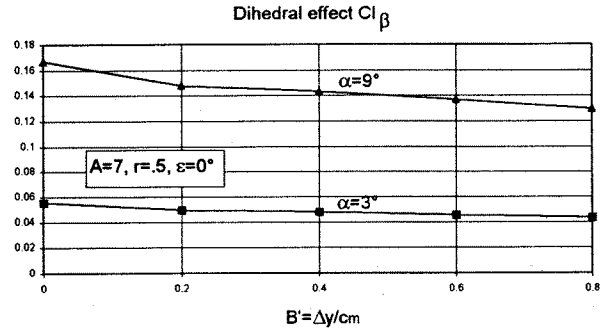

Figure 16: Variation of C_{l_β} for different wing tip shape at two angles of attack.

Conclusions

It is now possible to use a calculation program in order to determine the contribution to C_{l_β} for every straight wing, which are anyway tapered, twisted and rounded at the tip. The results above are quite satisfactory, though the references are too few to be compared. In fact, in [10] the diagrams are provided in order to determine the contribution to C_{l_β} for swept-tapered wings, which are relative to different aspect ratios and sweep-back angles, but this is not our case; moreover, on [2] the wing contribution to the C_{l_β} concerns an aircraft with very special features.

We intend to carry out a test in the wind tunnel of our Department at the Polytechnic of Turin on a isolated straight and swept-tapered wing. In this way we will obtain an immediate confirmation of the accuracy of our results, as well as an indication of the possible variation range of the involved parameters, in such a way to provide a constant precision of the results. We also intend to carry out tests on the same type of wings and with the same purposes: we will also use the whirling arm of the *Study Center for the Fluid Dynamics* of the CNR, which is guest in our Department.

The next development of this work will consist in the attempt to extend this method to swept wing with dihedral angle. This way we will be able to determine all the contributions of the wing to the dihedral effect and to consider wings of any shape and geometry.

List of Symbols

A	Aspect ratio
b	Wing span
$c(y)$	Local chord
c_l	Section lift coefficient
c_m	Mean geometric chord
c_r	Wing root chord
c_t	Wing tip chord
C_l	Rolling moment coefficient
C_{l_β}	Dihedral effect $= \partial C_l / \partial \beta$
C_L	Wing lift coefficient
L	Rolling moment
m_o	Wing section lift curve slope [1/rad]
r	Wing taper ratio $= c_t/c_r$
$\vec{r}$	Distance of P from vortex
s	Vortex co-ordinate
S	Wing area
V	Wind speed $= V_\infty$
V_i	Induced air speed
x, y, z	Body axes
y	Generic co-ordinate of a wing section $= b/2 \cos\theta$
y'	Vortex co-ordinate
α_a	Section apparent angle of attack
α_{as}	Absolute wing angle of attack measured from the zero lift direction of the root section
α_e	Section effective angle of attack
α_i	Section induced angle of attack
β	Sideslip angle
γ	Dihedral wing angle
$\Gamma(y)$	Circulation alon the wing span
ε^{rad}	Twist in radiants from root to tip
θ	Anomaly
Λ	Swept wing angle
ρ	Air density
σ	Vortex section

References

[1] R.F. Anderson, *Determination of the Characteristics of Tapered Wings*, NACA TR 572, 1936.

[2] H. Chester, B.Y. Roxanah, Wolowicz, *Lateral-Directional Aerodynamic Characteristics of Light, Twin-Engine, Propeller-Driven Airplanes*, NASA TN D-6946, 1972.

[3] S. D'Angelo, P.A. Gili, *Influenza della Configurazione di un Deltaplano sulle sue Qualità di Volo*, XI National Congress AIDAA, Forlì - Italy, 14/18 October, 1991.

[4] B. Etkin, *Dynamics of Flight - Stability and Control*, John Wiley & Sons, New York, Second edition, 1982.

[5] P. Gili, *The Sweep-Back Angle and the Aerodynamic Induction Like Wing Contributions to the Dihedral Effect*, 19th ICAS '94, Anaheim, CA - USA, 18/23 Sptember, 1994.

[6] A. Lausetti, F. Filippi, *Elementi di Meccanica del Volo*, Levrotto & Bella, Torino, 1956.

[7] R. Marini di Villafranca, *Aerodinamica dell'Ala in Basso Subsonico*, Giorgio Editore, Torino, 1971.

[8] C.D. Perkins and R.E. Hage, *Airplane Performance Stability and Control*, John Wiley & Sons, New York, 1949.

[9] F. Quori, *Aerodinamica*, Levrotto & Bella, Torino, Sett. 1993.

[10] Royal Aeronautical Society, *Data Sheet Aircraft*, 06. 01. 04.